SPE-187065-MS

On the Klinkenberg Effect of Multicomponent Gases

Shihao Wang, Colorado School of Mines; Zhengfu Pan and Juncheng Zhang, CCDC Downhole Service Co; Zhenzhou Yang and Yonghong Wang, CNPC; Yu-Shu Wu and Xiaopeng Li, Colorado School of Mines; Alexander Lukyanov, Delft University of Technology

This paper was prepared for presentation at the SPE Annual Technical Conference and Exhibition held in San Antonio, Texas, USA, 9-11 October 2017.

Abstract

In unconventional gas formations, due to the narrow pore size, gas molecules slip at the wall of the pore, known as the Klinkenberg effect. Although the Klinkenberg effect of single component gas has been thoroughly investigated, an accurate correlation for Klinkenberg effects on multicomponent gas flow has not been formulated so far. In this paper, we aim to quantify the multicomponent gas Klinkenberg effect by deriving a non-empirical correlation that can be directly used in reservoir engineering applications.

Our approach is based on kinetic theory, we calculate the mean free path of gas mixtures, and capture the loss of horizontal flux momentum of gas flux after the molecule diffusively reflect at the wall. The horizontal flux momentum acts as shear stress on gas flow. In this sense, the loss of momentum induces reduction of viscosity and enhancement of permeability (mass transfer). By quantifying the loss of horizontal momentum as well as the reduction of viscosity, we can solve the gas slippage coefficient for the multicomponent gas flow system.

We have brought out a second-order non-empirical gas slippage correlation for the multicomponent Klinkenberg effect problem. Our model well captures the mass transfer mechanism of gas mixtures. The accuracy of our model has been compared to and validated by both molecular dynamics simulation and physical experimental (tube-flooding). We have also investigated the effect of wall roughness on the reflection of gas molecules, which fundamentally reveals the origin of gas slippage effect. Our correlation can be readily implemented in compositional reservoir simulators to investigate gas flow in unconventional formations, such as shale and tight sandstone.

Compared to existing approaches, our approach has several novelties and advantages. First, our approach is a non-empirical gas slippage correlation for gas mixtures. The model is based on the kinetic theory of gasses, originating from the first principals. Secondly, our model is capable of handling a wide range of Knudsen numbers. Last, compared to Direct Simulation Monte Carlo (DSMC) and Lattice Boltzmann Method (LBM), our approach requires much less computing resources.

Introduction

As discovered by Maxwell (1879), when gas flows through narrow channels, the mass transfer rate increases due to momentum loss on the channel wall. The ratio between mean free path (average distance that a gas

molecular can move without any collisions) and the flow channel diameter is defined as Knudsen number, which quantifies the magnitude of the mass transfer enhancement effect. Maxwell (1879) brought out the very first slippage boundary condition, as shown in Equation (1)

$$u_{slip} = \frac{2}{3}\frac{2-\sigma}{\sigma}\cdot\lambda\left(\frac{\partial u}{\partial n}\right)_s \tag{1}$$

In this equation, u is the flux velocity at the boundary, σ is the Tangential Momentum Accommodation Coefficient (TMAC), which quantifies the ratio of momentum transfer on the boundarym and λ is the mean free path of the gas. The detailed explanations of symbols used in this paper can be found in the Nomenclature list. A general form of the slippage boundary condition can be expressed as

$$u_{slip} = C_1(K_N)\cdot\lambda\left(\frac{\partial u}{\partial n}\right)_s - C_2(K_N)\cdot\lambda^2\left(\frac{\partial^2 u}{\partial n^2}\right)_s \ldots \tag{2}$$

As shown in Equation (2), the boundary slippage velocity is a multiple order function of the velocity gradient. In Equation (2), the term C_1 and C_2 are the coefficients of first-order velocity gradient and second-order velocity gradient, respectively. By comparing Equation (1) and (2), it can be seen that Maxwell's slippage boundary condition is a first-order boundary condition with a constant coefficient. The pores' diameters of unconventional formation rock are ranging from several micrometers to several nanometers and can be viewed also as narrow channels. Therefore, gas mass transfer rate may also increse in unconventioanal reservois. Actually, the gas apparent permeability enhancement effect has been observed (Civan, 2010) during the investigation of unconventional resources. Klinkenberg firstly discovered the permeability enhancement effect in porous media and brought out a general model to quantify such effect, which was later named after him, as shown in Equation (3).

$$K_a = K_\infty\left(1+\frac{b}{P}\right) \tag{3}$$

In the above equation, b is an empirical parameter. Since $\lambda \propto 1/p$, Klinkenberg's correlation can be viewed as an empirical first-order slippage model.

Ever since Klinkenberg's work, many researchers have addressed this problem in both micro-scale and reservoir scale (Jiang et al., 2016; Wang et al., 2016; Wu et al., 2014), as summarized by (Zhang et al., 2012).

Knudsen (1934, 1909) investigated the diffusion effect induced by molecular-wall interaction for high Knudsen numbers and brought out the Knudsen diffusion effect along with the Knudsen diffusion coefficient. Pollard and Present (1948) later considered the gas diffusion in a long channel. According to Pollard and Present (1948)'s model, Knudsen diffusion coefficient is the 'extreme' value for very high Knudsen numbers (extremely narrow flow channel). The diffusion coefficient decreases from Knudsen diffusion coefficient continuously to molecular diffusion coefficient as the Knudsen number decreases from infinitely large to infinitely small. Javadpour (2009) presented an empirical correlation for the apparent gas permeability of unconventional rocks based on experimental data. Lasseux et al. (2016) combined Navier-Stokes equations with a first-order slippage condition to derive an analytical solution of the apparent gas permeability with respect to pressure. Wu and Bogy (2003) used gas kinetic theory to address this problem and derived a simple yet accurate second-order model for Knudsen number that is below *1*. Wu and Bogy (2003) considered the momentum loss on the pore wall. The model was later extended to higher Knudsen numbers (Wu, 2008). (Ohwada and Xu (2004) combined gas-kinetic scheme with Burnett equation to solve for the velocity profile as well as pressure/temperature distribution of gas flow inside microchannels. Wu et al. (2017) showed this work is only valid for low Knudsen numbers.

Recently, Wang et al. (2017a) presented a novel second-order slippage model, which accurately calculates the mass transfer enhancement in micro-channels and matches the numerical results (Li et al., 2011) as well

physical experiment (Colin et al., 2004) data very well. Wang et al. (2017) have thoroughly reviewed the fundamental theory as well as the applications of the gas transport mechanism in unconventional reservoirs.

Although the slippage model of single component gas flow has been investigated in-depth, the slippage model for multicomponent gas mixtures, however, has not been well developed yet. In this work, we proposed a non-empirical gas slippage for multicomponent gas mixtures. Our work is based on the published research (Wang et al., 2017a; Wu, 2008; Wu and Bogy, 2003) about single gas slippage. The proposed model can be conveniently implemented in reservoir simulator (Jiang, 2013; Li et al., 2016; Wang et al., 2017b; Wang et al., 2014) or well testing software to conduct production performance evaluation of unconventional gas reservoirs.

This paper is organized as follows. In Section 2, we briefly introduce the background of the kinetic theory of gases. In Section 3, we present the derivation of the proposed slippage model. In Section. 4, we show the permeability enhancement factor predicted by our model. In the last Section, we conclude this work and suggest for future work.

Background

Mean free path of gas mixture

By definition, the mean free path is the 'average' distance that a gas molecule can travel before it hits another gas molecule. The mean free path of gas can be calculated in several ways, resulting in slightly different values (Bird and A., 1976; Chapman and Cowling, 1970; Present, 1958). In this work, we follow Kennard's method (1938) to calculate the mean free path of the *i*th component of the gas mixture as follows

$$\lambda_i = \left[\frac{\pi}{4} \sum_{j=1}^{N_C} n_j \left(\sigma_i + \sigma_j \right)^2 \left(1 + \frac{m_i}{m_j} \right)^{1/2} \right]^{-1} \tag{4}$$

In the above equation, n_j is the number density of the *i*th type of molecules.

The 'overall' mean free path of the gas mixture is defined as

$$\lambda_{fm} = \sum_{j=1}^{Nc} x_j \lambda_j \tag{5}$$

Here λ_{fm} is calculated via a simple mixing rule and is used only for the calculation of Knudsen number in order to make comparison easier. From λ_{fm}, we can define Knudsen number for gas mixture as

$$K_N = \frac{\lambda_{fm}}{d} \tag{6}$$

Diffusive reflection and momentum loss

The impinging molecules reflect on the wall of the porous media. A certain amount of reflections are specular, in which the molecules maintain their horizontal momentum. The rest of the molecules diffusively reflect into a random direction, causing a loss of momentum, as shown in Figure 1. The diffusive reflection can be analogous to light scattering on rough surfaces and can be quantified by the method proposed by Bennett and Porteus (1961), Davies (1954), and Harvey et al. (2012). The percentage of the loss of the momentum is defined as Tangential Momentum Accommodation Coefficient (TMAC), ranging from *0* to *1*. The rougher the surface is, the higher TMAC is.

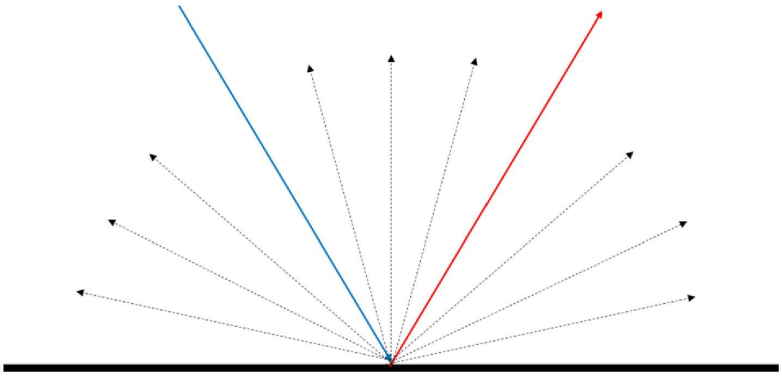

Figure 1—Conceptual model of gas molecular reflection on the rough surface (wall) of porous media. The solid arrow line represents the specular reflection, while the dash arrow lines represent the diffusive reflection.

The diffusively reflected molecules will lose their horizontal momentum after the reflection. Since the momentum gradient is the origin of shear stress, the loss of horizontal momentum will reduce the shear stress and thus reduce the viscosity of fluid that is in the vicinity of the pore wall, causing the fluid to 'slip.' In this work, we aim to quantify the slippage effect by quantifying the amount of loss momentum.

Kinetic theory of gasses and viscosity of gas mixtures

Consider a spherical coordinate system in which a small volume $d\tau$ of the gas is in a position (r,φ,ω), as shown in Figure 2. According to the kinetic theory of gasses (Present, 1958), in unit time the number of the ith type of molecules that collide once in $d\tau$, then leave $d\tau$ and reach a small area dS at (0,0,0) without any other collisions is

$$dN_i = x_i \frac{\bar{v}_i n \cdot d\tau}{\lambda_i} \frac{\cos\varphi}{4\pi r^2} \exp\left(-\frac{r}{\lambda_i}\right) \cdot dS \tag{7}$$

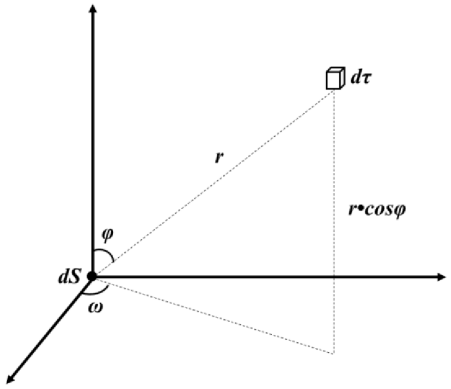

Figure 2—Coordinate system showing the relative position of *dS* and *dt*.

In the above formulation, x_i is the mole concentration of component i. n is the number density of the gas mixture. r is the traveling distance.

Moreover, from a certain direction, the average moving distance of the ith type of molecules is its mean free path λ_i. The average momentum the molecules tranport can be calculated by multiplying their flux velocity (in the mean moving distance controlled by mean free path) by their number density and mass.

For laminar flow (along x direction as shown in Figure 3), suppose there is no wall and no boundary reflection, then given an imaginary plain at $z = z_0$ with unit area in the space, all molecules that impinge into the unit area from φ direction in average carry the flux velocity at $z = z_0 + \lambda_i \cos\varphi$, as shown in Figure 4. In this sense, considering the amount of momentum tranported by ith type of molecules impinge from above is

$$M_{ui} = x_i \frac{\overline{v}_i m_i n}{4\pi} \int_0^{2\pi} \int_0^{\pi/2} u\left(z_0 + \lambda_i \cos\varphi\right) \cos\varphi \sin\varphi d\varphi d\omega \tag{8}$$

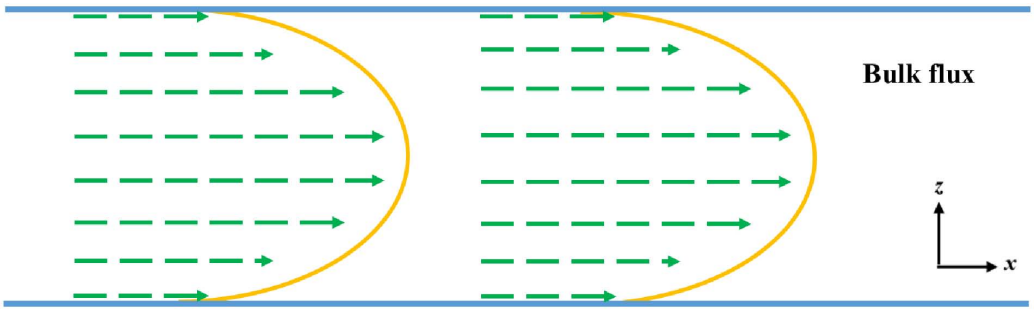

Figure 3—Conceptual model of laminar flow system.

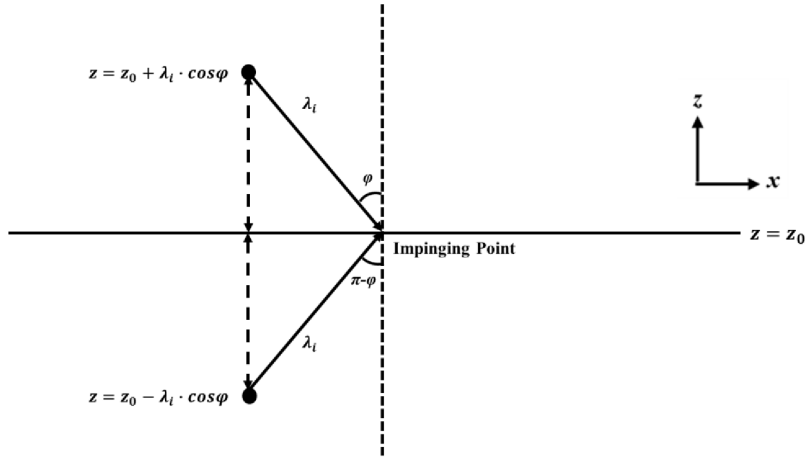

Figure 4—Conceptual model of the *i*th type of molecules that impinge into an imaginary plain in an open space within a laminar flow field. *x* direction is the flux direction, meaning that the flux velocity vector only has non-zero components along *x* direction.

In the above equation, u is the flux velocity. In the case of laminar flow, u is the function of z only. Similarly, the momentum carried by ith of molecules from bottom along direction (Π-φ) is

$$M_{bi} = x_i \frac{\overline{v}_i m_i n}{4\pi} \int_0^{2\pi} \int_0^{\pi/2} u\left(z_0 - \lambda_i \cos\varphi\right) \cos\varphi \sin\varphi d\varphi d\omega \tag{9}$$

Then, by summing up all N_C types of molecules, the total momentum from above direction and bellow direction can be calculated and expanded into second-order in (10) and (11), respectively.

$$\begin{aligned} M_u &= \sum_{i=1}^{N_C} M_{ui} = \sum_{i=1}^{N_C} x_i \frac{\overline{v}_i m_i n}{4\pi} \int_0^{2\pi} \int_0^{\pi/2} u\left(z_0 + \lambda_i \cos\varphi\right) \cos\varphi \sin\varphi d\varphi d\omega \\ &= \sum_{i=1}^{N_C} x_i \frac{\overline{v}_i m_i n}{4\pi} \int_0^{2\pi} \int_0^{\pi/2} \left[u\Big|_{z_0} + \lambda_i \cos\varphi \left(\frac{\partial u}{\partial z}\right)\Big|_{z_0} + \frac{1}{2}\lambda_i^2 \cos^2\varphi \left(\frac{\partial^2 u}{\partial z^2}\right)\Big|_{z_0} \right] \cos\varphi \sin\varphi d\varphi d\omega \end{aligned} \tag{10}$$

$$M_b = \sum_{i=1}^{N_C} M_{bi} = \sum_{i=1}^{N_C} x_i \frac{\overline{v}_i m_i n}{4\pi} \int_0^{2\pi} \int_0^{\pi/2} u\left(z_0 - \lambda_i \cos\varphi\right) \cos\varphi \sin\varphi d\varphi d\omega$$
$$= \sum_{i=1}^{N_C} x_i \frac{\overline{v}_i m_i n_i}{4\pi} \int_0^{2\pi} \int_0^{\pi/2} \left[u\big|_{z_0} - \lambda_i \cos\varphi \left(\frac{\partial u}{\partial z}\right)\Big|_{z_0} + \frac{1}{2}\lambda_i^2 \cos^2\varphi \left(\frac{\partial^2 u}{\partial z^2}\right)\Big|_{z_0} \right] \cos\varphi \sin\varphi d\varphi d\omega \quad (11)$$

The shear force on the plain is just the difference between M_u and M_b as

$$\tau = M_u - M_b = \frac{1}{3} \sum_{i=1}^{N_C} x_i \overline{v}_i m_i n \lambda_i \left(\frac{\partial u}{\partial z}\right)\Big|_{z_0} \quad (12)$$

Based on the definition of viscosity, we can obtain the viscosity of gas mixture as

$$\mu_{ideal} = \frac{1}{3} \sum_{i=1}^{N_C} x_i \overline{v}_i m_i n \lambda_i \quad (13)$$

In this sense, we can use this mean free path method originated from the kinetic theory of gases to estimate the viscosity of ideal gas mixtures. Based on this model, we can further calculate the slippage boundary condition of gas mixtures by putting the mixture into a confined flow channel.

Non-empirical slippage model

In this Section, we present the derivation of our non-empirical gas slippage model of gas mixtures. As mentioned in the previous Sections, the existence of walls and diffusive reflection is the origin of viscosity reduction as well as boundary slippage. Consider a bunch of molecules that impinge in a point (unit area) on the boundary ($z=0$) along direction φ, as shown in Figure 5.

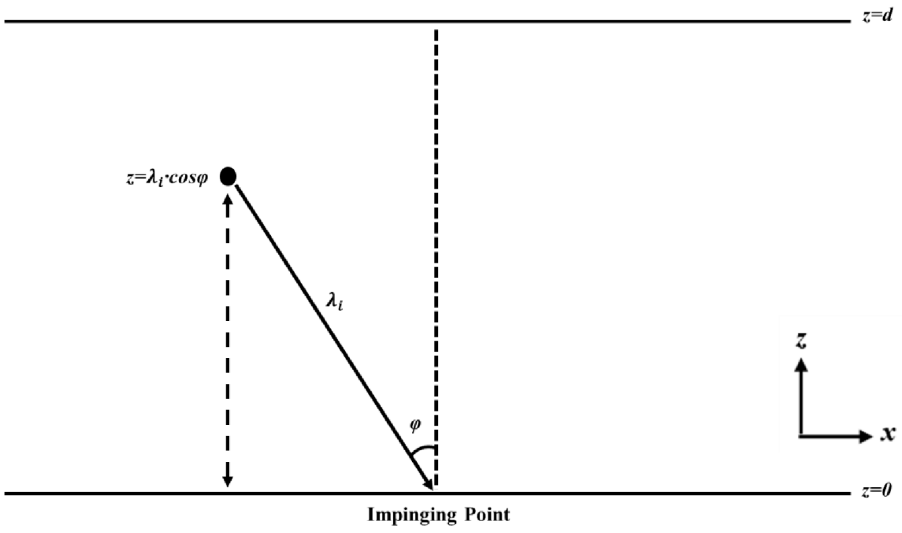

Figure 5—Conceptual model of momentum loss on the boundary.

According to our previous discussion, the average flux velocity these molecules carry is the flux velocity at $z = \lambda_i \cos\varphi$. Moreover, only diffusively reflection contribute to the net momentum transfer. Therefore, all the '*effective*' momentum transported by all types of molecules can be calculated as

$$M_w = \sigma \sum_{i=1}^{N_C} M_{wi} = \sigma \sum_{i=1}^{N_C} x_i \frac{\overline{v}_i m_i n}{4\pi} \int_0^{2\pi} \int_0^{\pi/2} u\left(\lambda_i \cos\varphi\right) \cos\varphi \sin\varphi d\varphi d\omega \quad (14)$$

The above formulation can be expanded to the second order as

$$M_{wi}=\sum_{i=1}^{N_C}x_i\frac{\overline{v}_i m_i n}{4\pi}\int_0^{2\pi}\int_0^{\pi/2}\left[u\big|_w+\lambda_i\cos\varphi\left(\frac{\partial u}{\partial z}\right)\Big|_w+\frac{1}{2}\lambda_i^2\cos^2\varphi\left(\frac{\partial^2 u}{\partial z^2}\right)\Big|_w\right]\cos\varphi\sin\varphi d\varphi d\omega \tag{15}$$

Equation (15) is the actual momentum transfer on the wall. By equating Equation (15) with Equation (13), we can obtain the 'equivalent' slippage velocity that generates the apparent permeability, as shown in

$$\sigma\sum_{i=1}^{N_C}x_i\frac{\overline{v}_i m_i n}{2}\left[\frac{1}{2}u\big|_w+\frac{1}{3}\lambda_i\left(\frac{\partial u}{\partial z}\right)\Big|_w+\frac{1}{8}\lambda_i^2\left(\frac{\partial^2 u}{\partial z^2}\right)\Big|_w\right]=\sum_{i=1}^{N_C}x_i\frac{\overline{v}_i m_i n}{3}\lambda_i\left(\frac{\partial u}{\partial z}\right)\Big|_w \tag{16}$$

By reorganizing the above equation, the slippage velocity correlation can be obtained as

$$u\big|_w=\frac{2}{3}\frac{2-\sigma}{\sigma}\left(\frac{\partial u}{\partial z}\right)\Big|_w\frac{\sum_{i=1}^{N_C}x_i\overline{v}_i\lambda_i}{\sum_{i=1}^{N_C}x_i\overline{v}_i}-\frac{1}{4}\left(\frac{\partial^2 u}{\partial z^2}\right)\Big|_w\frac{\sum_{i=1}^{N_C}x_i\overline{v}_i\lambda_i^2}{\sum_{i=1}^{N_C}x_i\overline{v}_i} \tag{17}$$

Consider $\overline{v}_i\propto(\sqrt{m_i})^{-1}$, then the slippage velocity can be expressed as

$$u\big|_w=\frac{2}{3}\frac{2-\sigma}{\sigma}\frac{\sum_{i=1}^{N_C}\frac{x_i}{\sqrt{m_i}}\lambda_i}{\sum_{i=1}^{N_C}\frac{x_i}{\sqrt{m_i}}}\left(\frac{\partial u}{\partial z}\right)\Big|_w-\frac{1}{4}\frac{\sum_{i=1}^{N_C}\frac{x_i}{\sqrt{m_i}}\lambda_i^2}{\sum_{i=1}^{N_C}\frac{x_i}{\sqrt{m_i}}}\left(\frac{\partial^2 u}{\partial z^2}\right)\Big|_w \tag{18}$$

Compared with Equation (2), the two coefficients C_1 and C_2 in our model are as follows

$$C_1=\frac{2}{3}\frac{2-\sigma}{\sigma}\frac{\sum_{i=1}^{Nc}\frac{x_i}{\sqrt{m_i}}\lambda_i}{\sum_{j=1}^{Nc}\frac{x_j}{\sqrt{m_j}}\bullet\sum_{k=1}^{Nc}x_k\lambda_k} \tag{19}$$

$$C_2=\frac{1}{4}\frac{\sum_{i=1}^{Nc}\frac{x_i}{\sqrt{m_i}}\lambda_i^2}{\sum_{j=1}^{Nc}\frac{x_j}{\sqrt{m_j}}\bullet\left(\sum_{k=1}^{Nc}x_k\lambda_k\right)^2} \tag{20}$$

Moreover, it can be easily seen that for single component gas flow at very low Knudsen number, this newly proposed model reduces to Maxwell's one, in Equation (1).

Results and validation

Validation

We use Li et al's (2011) results to validate our results for the single-component case. Li et al. (2011) used Lattice Boltzmann Method (LBM) to simulate gas transport in microchannels. In their work, they consider purely diffusive reflection (TMAC=1). In this paper, we compared the dimensionless flow rate Q_D predicted

by Li et al. (2011)'s model and our non-empirical correction. The dimensionless flow rate is defined as follows

$$Q_D = -\int_0^h \rho u dz \sqrt{2RT} \,/\, \left(h^2 \,\partial p/\partial x\right) \tag{21}$$

For our proposed correlation, Q_D can be explicitly expressed as

$$Q_D = \frac{\sqrt{\pi}}{12K_N} + \frac{\sqrt{\pi}}{2} C_1 + \sqrt{\pi} K_N C_2 \tag{22}$$

The comparison is shown in Figure 6, from which it can be seen that the proposed model matches numerical experimental results very well.

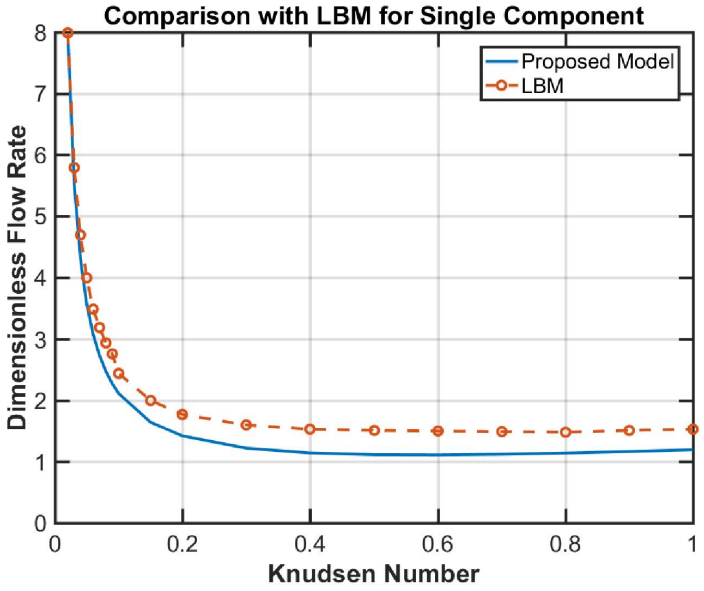

Figure 6—Comparison between LBM results and proposed kinetic model for single component gas flow with TMAC being 1.

Results

In this section, we present the permeability enhancement factor of a binary gas mixture as well as a ternary gas mixture predicted by our proposed correlation. The permeability enhancement factor can be calculated analytically by our model, as shown in the equation below.

$$S = 1 + 6C_1 K_N + 12C_2 K_N^2 \tag{23}$$

Binary gas mixture. Here we present the impact of compositional distribution on the permeability enhancement factor of binary gas mixtures. For gas mixtures, their mean free path is the function of both temperature/pressure and the compositional distribution of their components. The summary of the compositional combinations of the binary gas mixtures is listed in Table 1. In this work, we use real gas properties to calculate the mean free path as well as the permeability enhancement factor. The temperature is set to be *212 °F* (*373 K*). The 'average' mean free path of the gas mixture that has 50% methane and 50% propane is shown in Figure 7. In Figure 7, we also plot the mean free path of methane molecules and propane molecules within the mixture. The steep portion of the mean free path curve of propane refers to the transition from gas phase to super-critical phase. The mean free path of 70% methane-30% propane mixture is shown in Figure 8. The permeability enhancement factor with respect to pressure for a 25nm wide channel and a 15nm wide channel is shown in Figure 9 and Figure 10. respectively. From the two

figures, it can be seen that the permeability enhancement effect of a binary mixture can be significantly different from that of one pure component.

Table 1—Summary of concentration combinations of binary mixture cases.

	Methane	Propane
Case 1	100%	0%
Case 2	70%	30%
Case 3	50%	50%
Case 4	30%	70%
Case 5	0%	100%

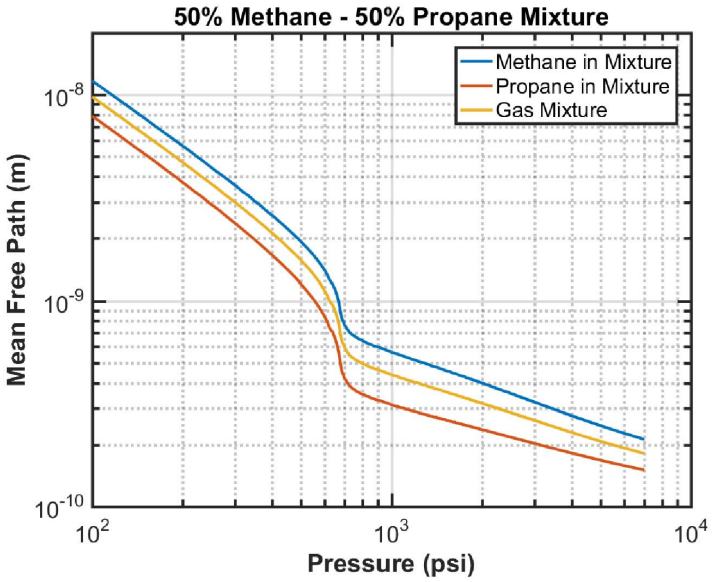

Figure 7—Mean free path of 50% methane-50% propane mixture. The temperature is 212 °F (373 K).

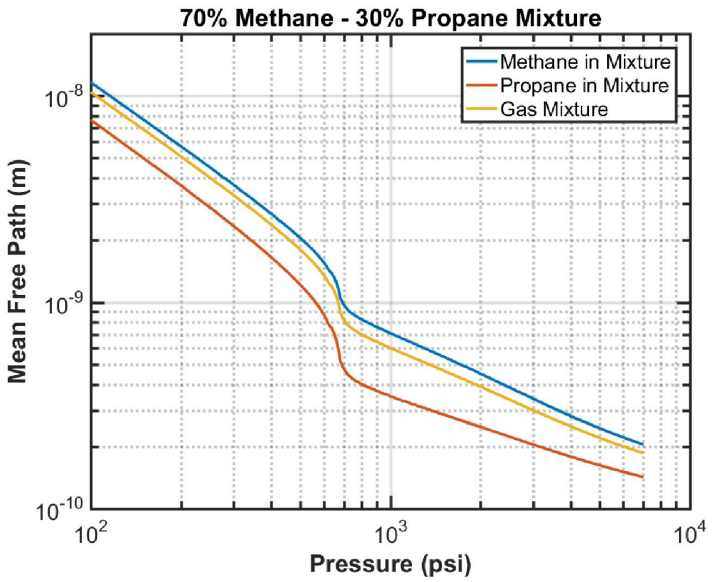

Figure 8—Mean free path of 70% methane-30% propane mixture. The temperature is 212 °F (373 K).

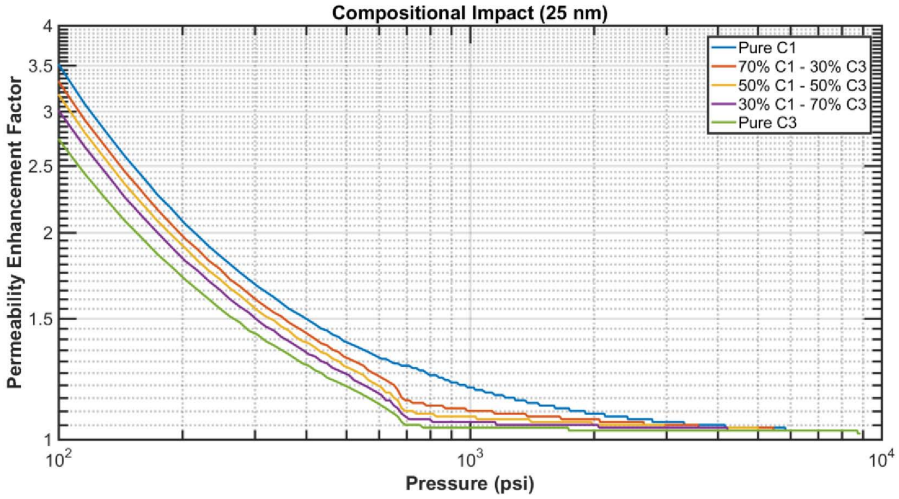

Figure 9—Permeability enhancement factor for different composition distribution of methane-propane mixtures within 25nm channel with respect to pressure.

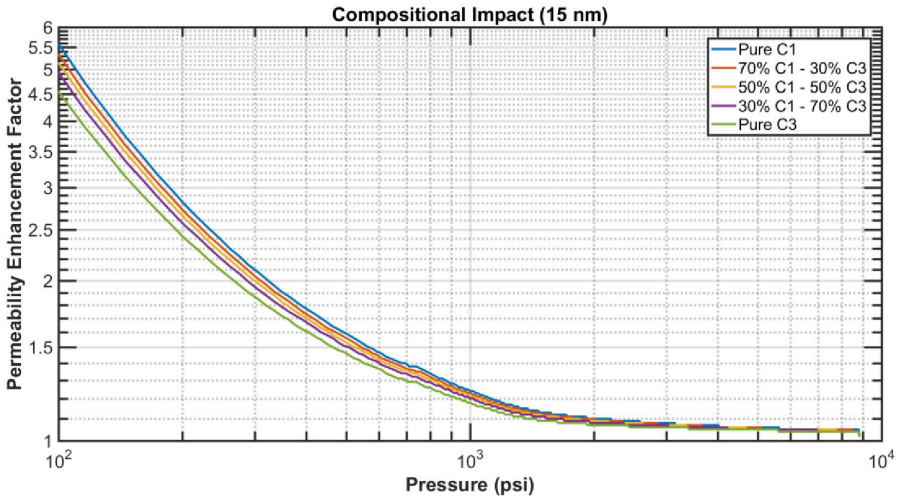

Figure 10—Permeability enhancement factor for different composition distribution of methane-propane mixtures within 15nm channel with respect to pressure. Both of the two axes are in log scale.

Ternary gas mixture. In this sub-section, we discuss the impact of compositional distribution on the permeability enhancement factor of a ternary gas mixture. The summary of the compositional combinations is listed in Table 2. The permeability enhancement factor with respect to pressure for the 25nm wide channel and the 15nm wide channel is shown in Figure 11 and Figure 12, respectively. From the two figures, we can see that our proposed correlation is able to capture the compositional impact for ternary gas mixtures. Moreover, there should be little difficulty for our correlation to predict the permeability enhancement effect of more complex gas mixtures consisting of light components.

Table 2—Summary of concentration combinations of ternary mixture cases.

	Methane	Ethane	Propane
Case 6	10%	20%	70%
Case 7	33.3%	33.3%	33.3%
Case 8	70%	20%	10%

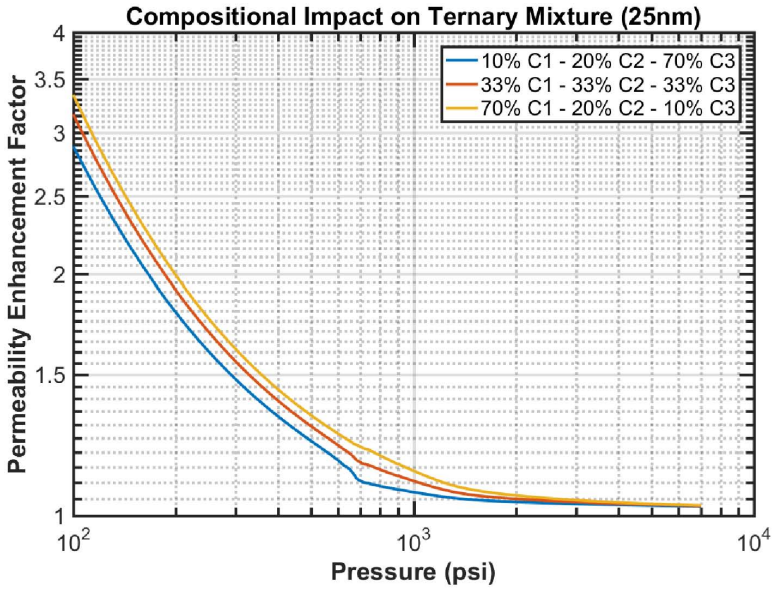

Figure 11—Permeability enhancement factor for different composition distribution of methane-ethane-propane mixtures within 25nm channel with respect to pressure. Both of the two axes are in log scale.

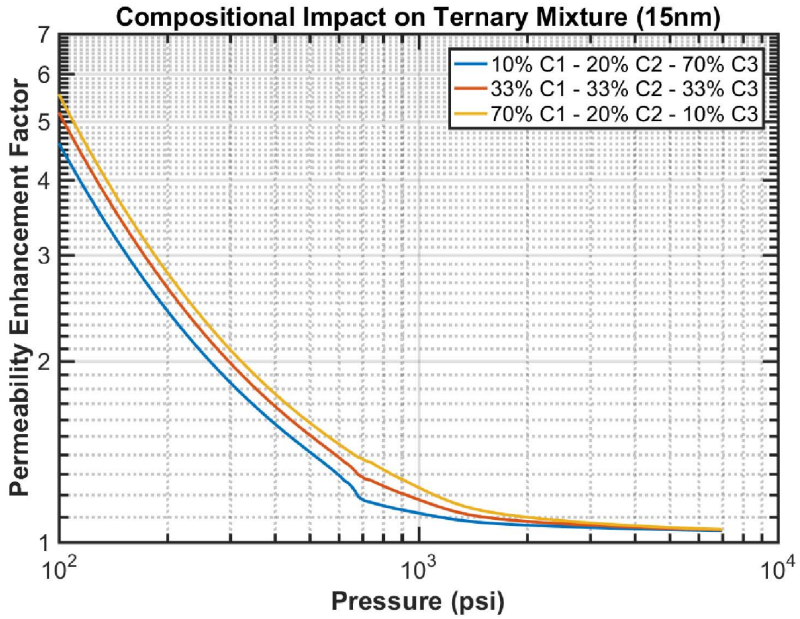

Figure 12—Permeability enhancement factor for different composition distribution of methane-ethane-propane mixtures within 15nm channel with respect to pressure. Both of the two axes are in log scale.

Summary and discussion

To sum up, in this work, we have derive a novel non-empirical model to quantify the Klinkenberg effect for multicomponent gas mixtures. Based on the kinetic theory of gases, our model has a solid physical foundation. It has been validated against molecular simulation results and has shown good accuracy for low to moderate Knudsen numbers ($K_N < 1$). For higher Knudsen numbers, our model may show larger errors.

Using the proposed model, we have investigated the Klinkenberg effect of binary as well ternary gas mixtures. We found that heavier components inside the gas mixture can significantly vary the slippage behaviors of the mixture. Moreover, the slippage behaviors also depend on the compositional distribution. Lighter components contribute to more slippage effect.

Admittedly, our model has several limitations. First, it can only be used to low-speed gas flow, because it assumes near-steady conditions in its derivation. Secondly, it should only be applied to gas reservoirs with mostly light components. For gas mixtures with heavier components, for instance condensate gas reservoirs, complex phase behaviors may involve during the recovery process, which may cause the failure of our model.

To the best our knowledge, this work is the first non-empirical correlation for gas mixtures in this area. It is promising that our proposed model will be adopted and applied to reservoir simulation of unconventional gas formations.

Acknowledgement

This work was supported by the CNPC-USA and Foundation CMG.

Nomenclature

b	Klinkenberg factor
D	pore diameter
i	component index
j	component index
K_∞	absolute permeability
K_a	apparent permeability
K_N	Knudsen number
m	molecular weight
N	number density
Q_D	dimensionless flow rate
P	pressure
R	gas constant
S	permeability enhancement factor
T	temperature
δ	collision diamter
u	flux velocity
τ	unit volume
v	thermal velocity
x	horizontal dimension
z	vertical dimension
φ	spherical angle
ω	radial angle
λ	mean free path
ρ	density
σ	Tangential Momentum Accommodation Coefficient (TMAC)

Reference

Bennett, H.E., Porteus, J.O., 1961. Relation Between Surface Roughness and Specular Reflectance at Normal Incidence. *J. Opt. Soc. Am*. **51**, 123. doi: 10.1364/JOSA.51.000123

Bird, G.A., A., G., 1976. Molecular gas dynamics, Research supported by the U.S. Air Force; Oxford, Clarendon Press, 1976. 250 p. Oxford.

Chapman, S., Cowling, T.G. (Thomas G., 1970. The mathematical theory of non-uniform gases; an account of the kinetic theory of viscosity, thermal conduction and diffusion in gases. Cambridge University Press.

Civan, F., 2010. Effective Correlation of Apparent Gas Permeability in Tight Porous Media. *Transp. Porous Media* **82**, 375–384. doi:10.1007/s11242-009-9432-z

Colin, S., Lalonde, P., Caen, R., 2004. Validation of a second-order slip flow model in rectangular microchannels. *Heat Transf. Eng*. **25**, 23–30. doi:10.1080/01457630490280047

Davies, H., 1954. The reflection of electromagnetic waves from a rough surface. *Proc. IEE - Part IV Inst. Monogr*. **101**, 209–214. doi:10.1049/pi-4.1954.0025

Harvey, J.E., Schröder, S., Choi, N., Duparré, A., 2012. Total integrated scatter from surfaces with arbitrary roughness, correlation widths, and incident angles. *Opt. Eng*. **51**, 13402. doi: 10.1117/1.OE.51.1.013402

Javadpour, F., 2009. Nanopores and Apparent Permeability of Gas Flow in Mudrocks (Shales and Siltstone). *J. Can. Pet. Technol*. **48**, 16–21. doi:10.2118/09-08-16-DA

Jiang, R., 2013. PRESSURE PRECONDITIONING USING PROPER. Stanford University.

Jiang, R., Stern, D., Halsey, T.C., Manzocchi, T., 2016. SCENARIO DISCOVERY WORKFLOW FOR ROBUST PETROLEUM RESERVOIR DEVELOPMENT UNDER UNCERTAINTY. *Int. J. Uncertain. Quantif*. **6**, 533–559. doi:10.1615/Int.J.UncertaintyQuantification.2016018932

Kennard, E., 1938. Kinetic theory of gases, 1st ed. McGraw-Hill Book Co, New York and London.

Knudsen, M., 1934. The Kinetic Theory of Gases. Methuen & Co. Ltd., London.

Knudsen, M., 1909. Die Gesetze der Molekularströmung und der inneren Reibungsströmung der Gase durch Röhren. *Ann. Phys*. **333**, 75–130. doi:10.1002/andp.19093330106

Lasseux, D., Valdés Parada, F.J., Porter, M.L., 2016. An improved macroscale model for gas slip flow in porous media. *J. Fluid Mech*. **805**, 118–146. doi:10.1017/jfm.2016.562

Li, Q., He, Y.L., Tang, G.H., Tao, W.Q., 2011. Lattice Boltzmann modeling of microchannel flows in the transition flow regime. *Microfluid. Nanofluidics* **10**, 607–618. doi:10.1007/s10404-010-0693-1

Li, X., Abass, H., Teklu, T.W., Cui, Q., 2016. A Shale Matrix Imbibition Model and Interplay between Capillary Pressure and Osmotic Pressure, in: SPE Annual Technical Conference and Exhibition. Society of Petroleum Engineers. doi: 10.2118/181407-MS

Maxwell, C., 1879. On Stresses in Rarified Gases Arising from Inequalities of Temperature on JSTOR. *Philos. Trans. R. Soc. London* **170**, 231–256. doi:10.1098/rstl.1879.006

Ohwada, T., Xu, K., 2004. The kinetic scheme for the full-Burnett equations. *J. Comput. Phys*. **201**, 315–332. doi:10.1016/j.jcp.2004.05.017

Pollard, W.G., Present, R.D., 1948. On Gaseous Self-Diffusion in Long Capillary Tubes. *Phys. Rev*. **73**, 762–774. doi:10.1103/PhysRev.73.762

Present, R.D., 1958. Kinetic Theory of Gases. McGraw-Hill.

Wang, L., Wang, S., Zhang, R., Wang, C., Xiong, Y., Zheng, X., Li, S., Jin, K., Rui, Z., 2017. Review of multi-scale and multi-physical simulation technologies for shale and tight gas reservoirs. *J. Nat. Gas Sci. Eng*. **37**, 560–578. doi:10.1016/j.jngse.2016.11.051

Wang, S., Huang, Z., Wu, Y.-S., Winterfeld, P.H., Zerpa, L.E., 2016. A semi-analytical correlation of thermal-hydraulic-mechanical behavior of fractures and its application to modeling reservoir scale cold water injection problems in enhanced geothermal reservoirs. *Geothermics* **64**, 81–95. doi:10.1016/j.geothermics.2016.04.005

Wang, S., Lukyanov, A.A., Wang, L., Wu, Y.-S., Pomerantz, A., Xu, W., Kleinberg, R., 2017a. A non-empirical gas slippage model for low to moderate Knudsen numbers. *Phys. Fluids* **29**, 12004. doi: 10.1063/1.4974319

Wang, S., Xiong, Y., Winterfeld, P., Zhang, K., Wu, Y.-S., 2014. Parallel Simulation of Thermal-Hydrological-Mechanic (THM) Processes in Geothermal Reservoirs, in: PROCEEDINGS of the 39th Workshop on Geothermal Reservoir Engineering. Stanford University, Stanford, California.

Wang, S., Zhang, J., Yang, Z., Yin, C., Wang, Y., Zhang, R., Winterfeld, P., Wu, Y.-S., 2017b. Fully Coupled Thermal-Hydraulic-Mechanical Reservoir Simulation with Non-Isothermal Multiphase Compositional Modeling, in: SPE Reservoir Simulation Conference. Society of Petroleum Engineers. doi: 10.2118/182595-MS

Wu, L., 2008. A slip model for rarefied gas flows at arbitrary Knudsen number. *Appl. Phys. Lett*. **93**, 1–4. doi:10.1063/1.3052923

Wu, L., Bogy, D.B., 2003. New First and Second Order Slip Models for the Compressible Reynolds Equation. *J. Tribol*. **125**, 558. doi: 10.1115/1.1538620

Wu, L., Ho, M.T., Germanou, L., Gu, X.-J., Liu, C., Xu, K., Zhang, Y., 2017. A comment on `An improved macroscale model for gas slip flow in porous media'.

Wu, Y.-S., Li, J., Ding, D., Wang, C., Di, Y., 2014. A Generalized Framework Model for the Simulation of Gas Production in Unconventional Gas Reservoirs. *SPE J*. **19**, 845–857. doi:10.2118/163609-PA

Zhang, W.M., Meng, G., Wei, X., 2012. A review on slip models for gas microflows. *Microfluid. Nanofluidics* **13**, 845–882. doi:10.1007/s10404-012-1012-9